Ultrasonics 128 (2023) 106885

Contents lists available at ScienceDirect

Ultrasonics

journal homepage: www.elsevier.com/locate/ultras

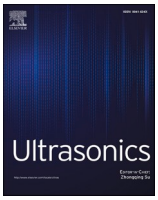

Numerical and experimental investigation of guided ultrasonic wave propagation in non-uniform plates with structural phase variations

Beata Zima [a,*], Jochen Moll [b]

[a] Faculty of Mechanical Engineering and Ship Technology, Gdańsk University of Technology, 80-233 Gdańsk, Poland
[b] Department of Physics, Goethe University Frankfurt, 60438 Frankfurt, Germany

ARTICLE INFO

Keywords:
Guided waves
Irregular plate with non-uniform thickness
Finite element simulations
Experimental testing
CNC manufacturing

ABSTRACT

The article presents the results of numerical and experimental investigations of guided wave propagation in aluminum plates with variable thickness. The shapes of plate surfaces have been specially designed and manufactured using a CNC milling machine. The shapes of the plates were defined by sinusoidal functions varying in phase shift, which forced the changes in thickness variability alongside the propagation path. The main aim of the study is to analyze the wave propagation characteristics caused by non-uniform thickness. In the first step, the influence of thickness variability on the time course of propagating waves has been analyzed theoretically. The study proves that the wave propagation signals can be determined based on knowledge about the statistical description of the specimen geometry. The histograms of thickness distribution together with the a priori knowledge of the dispersion curves were used to develop an iterative procedure assuming that the signal from the previous step becomes the excitation in the next step. Such an approach allowed for taking into account the complex geometry of the plate and rejecting the assumption about the constant average thickness alongside the propagation path. In consequence, it was possible to predict correctly the signal time course, as well as the time of flight and number of propagating wave modes in specimens with variable thickness. It is demonstrated that theoretical signals predicted in this way coincide well with numerical and experimental results. Moreover, the novel procedure allowed for the correct prediction of the occurrence of higher-order modes.

1. Introduction

In a variety of fields, from engineering to medical sciences, guided ultrasonic waves (GUW) are used to determine the properties of the medium in which they propagate [1]. In the simple case of a flat solid medium made of homogeneous, isotropic material, GUW modes propagate with the same velocity in each direction [2]. The so-called Lamb waves [3] become dispersive which means that their velocity and the number of triggered modes depend on the material parameters of the structure as well as the frequency-times-thickness product. The assumption that for a certain structure a unique set of dispersion curves can be traced was the foundation of many methods aimed at solving the inverse problems i.e. determining the parameters of the tested medium based on reconstructed dispersive curves [4,5]. In the majority of cases, the thickness was assumed to be constant which enables the application of the so far developed methods for diagnostics of more complex structures characterized by non-uniform geometry. Because the relation between velocity and plate thickness, as well as material parameters, is nonlinear, the assumption that the average velocity can be used to determine the average thickness leads to significant inaccuracies [6], especially in damage localization applications. Thus, for the further development of wave-based diagnostic procedures, it is important to take into account the possible thickness variability and its influence on signal characteristics.

The attempt of a theoretical description of wave propagation in specimens with variable thickness was made by Pageneux and Maurel [7]. The behavior of adiabatic modes in specimens with linearly varying thickness was investigated by El-Kettani et al. [8] and Moreau et al. [9]. Höhne [10,11] used a multimodal approach to simulate ultrasound propagation in cylindrical waveguides with non-constant thickness. The technique for pulse prediction and compensation in specimens with a variable cross-section was proposed by De Marchi et al. [12,13]. Guided waves in tapered waveguides were considered by Deng and Yang [14], Moll et al. [15] and Zima [16].

Despite the effort put into the analysis of wave propagation in plates with variable thickness, the detailed description of wave propagation in

* Corresponding author.
E-mail address: beata.zima@pg.edu.pl (B. Zima).

https://doi.org/10.1016/j.ultras.2022.106885
Received 6 June 2022; Received in revised form 22 August 2022; Accepted 27 October 2022
Available online 1 November 2022

plates with non-uniform geometry is still a research gap requiring consideration. The present study focuses on the analysis of the effects of smooth geometric thickness variations on wave propagation signals. The numerical and experimental investigations were conducted for sinusoidal-shaped plates varying in phase shift. In the first step, the influence of thickness variability on the time course of propagating waves has been analyzed theoretically. In the next steps, the time variability of wave propagation signals has been determined making use of a priori knowledge of the material parameters and dispersion relations The paper presents the novel procedure of signal reconstruction based only on statistical information about the geometry i.e. histograms of plate thickness distribution. The signal is obtained by using an iterative procedure based on assumption that the signal from the previous step becomes the excitation in the next step. The proposed method allowed for the prediction of the occurrence of higher-order modes, which can be useful in interpreting complex signals registered in objects with complicated non-uniform shapes.

The paper is organized as follows: the theoretical background is presented in Section 2. Materials and methods are described in Section 3, while the results are discussed in Section 4. Finally, the conclusions are drawn in Section 5.

2. Theoretical background

To consider the influence of thickness variability on wave propagation, let's consider the plate-like structure, depicted in Fig. 1. The time variability of guided wave $u(x_1,t)$ at the distance x_1 from the wave source after excitation defined as $F(\omega)$ in the frequency domain can be predicted based on the following expression:

$$u(x_1,t) = A(x_1)\int_{-\infty}^{\infty} F(\omega)e^{i(\omega t - k(\omega)x_1)}d\omega \tag{1}$$

where the factor $A(x_1)$ describes the amplitude decay and $k(\omega)$ is the wavenumber-frequency relationship. The above equation rewritten in the frequency domain takes the following form:

$$U(x_1,\omega) = U(0,\omega)e^{-ik(\omega)x_1} \tag{2}$$

Where $U(x,\omega)$ and $U(0,\omega)$ are the Fourier transforms of the received signal and the excitation, respectively.

Now, let's consider the time variability at the point located at the distance x_2 from the first point. The signal in point x_2 can be determined in two ways: by determining the waveform at the distance x_1+x_2 from the source or by treating the waveform registered in point x_1 as an excitation function:

$$U(x_2,\omega) = U(0,\omega)e^{-ik_1(\omega)x_1}e^{-ik_2(\omega)x_2} = U(0,\omega)e^{-i(k_1(\omega)x_1+ik_2(\omega)x_2)} \tag{3}$$

In both cases we obtain the same results which can be used to derive a more general form:

$$U(x_n,\omega) = U(0,\omega)e^{-i(\sum_{i=1}^{n}k_j(\omega)x_j)} \tag{4}$$

where n is the number of divisions alongside the plate. To take into account the possibility of propagation of several Lamb modes the equation can be written as follows:

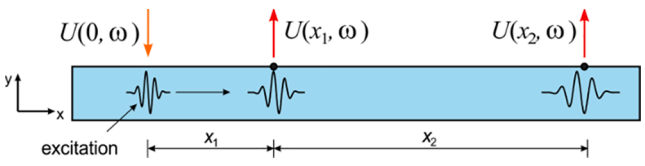

Fig. 1. Determining the time variability of the signal at different distances from the source.

$$U(x_n,\omega) = \sum_{i=1}^{N} U(0,\omega)e^{-i(\sum_{i=1}^{n}k_j^N(\omega)x_j)} \tag{5}$$

where N represents the number of Lamb modes. Based on the above derivations one can conclude that the shape of the wave packet depends on the thickness distribution along the propagation path but not on the exact shape of the plate. The same situation takes place in the case of the ToF of a wave passing through the distance L divided into n divisions with lengths Δx varying in thickness and thus, in wave velocityc_g:

$$ToF = \sum_{i=1}^{n}\frac{\Delta x}{c_{g_i}} \tag{6}$$

Its value is also independent of the geometry, but only on the thickness distribution.

3. Materials and methods

3.1. Experimental investigation

Computerized Numerical Control (CNC) was incorporated into the manufacturing procedure of experimental samples. Four solid plates considered here made of aluminum (elastic modulus $E = 70$ GPa, Poisson's ratio $\nu = 0.33$ and density $\rho = 2700$ kg/m^3) were characterized by specially designed sinusoidal shape. Both surfaces were defined by the same equation:

$$s(x) = a\cdot\sin(k_s x - \varphi) + h_0 \tag{7}$$

where a is the amplitude and k_s is the wavenumber related to plate shape and h_0 is the initial plate thickness.

The phase shift φ for the bottom surface each time was equal to 0 in all four cases, while for the upper surface this value varied from 0 toπ. The amplitude $a = 8$ mm, initial thickness $h_0 = 20$ mm and the wavenumber $k_s = 0.011$ rad/mm were established by taking into account the difference in wave velocity between particular plates as well as the technological possibilities of manufacturing. The total length L was 500 mm and was dictated by the size of the operating space of the CNC machine. In the case of plate#1 the phase shift was zero, both surfaces were described by the same function and thus, the plate thickness was constant. In the case of plate #4 the phase shift of the bottom surface was equal toπ, which forced the greatest thickness variability. Additionally, two intermediate cases were investigated ($\varphi = \pi/3$ and $\varphi = 2\pi/3$). The sinusoidal, smooth shape of the plates allowed for avoiding abrupt thickness changes associated with wave reflections and additional mode conversion. Because the geometry of each plate is defined by the same function and only the phase shift is variable, one can conclude that all differences in signals obtained for various plates result only from variable thickness, while not from the undesired effects related to the specific geometry of particular plates. The geometry, the histograms presenting thickness distributions, and the photos of investigated plates are given in Fig. 2.

Guided waves were excited and registered by rectangular piezoceramic transducers with dimensions of 30 × 5 mm manufactured by Physik Instrumente attached at both ends of each plate. To generate and register GUW the oscilloscope and function generator Handyscope HS5 (TiePie) was connected to a specially designed device Rammsbone [17]. The transducers were attached perpendicularly to the plate surface on top of the specimen. Thus, both mode families (symmetric and antisymmetric) were generated.

3.2. Numerical modeling

Numerical analysis was performed by using FEM-based software Abaqus/Explicit. Three-dimensional models were built of eight-node brick elements with reduced integration (C3D8R). The 3D model

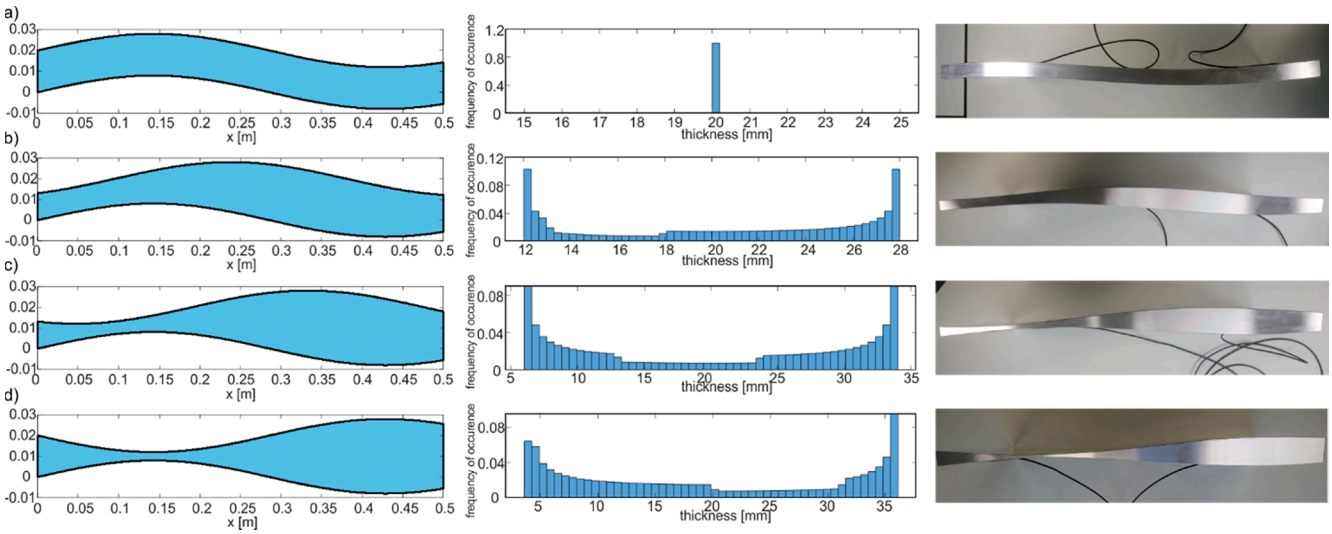

Fig. 2. Tested sine-shaped plates: a) plates geometry, b) thickness distributions and c) the photos of the specimens.

allowed for registering edge reflections in signals, which would not be possible in a less time-consuming plane strain model. The numerical investigation was preceded by an analysis of the dispersion curves for particular plates presented in the further part of the paper to adjust the mesh element size to recommendations saying that at least 10 nodes per wavelength should be used in a model [18,19]. The transient wave propagation problem was solved with an integration time step of 10^{-8} s, which was adjusted according to CFL condition for the frequency and wavelength [20]. The element size did not exceed 1 mm^3 and was established based on the results of the convergence study.

The excitation was applied as a time-dependent pressure applied on the area corresponding to the area of the real piezo transducers. The excitation function was in form of a five-cycle sine modulated by the Hann window:

$$p(t) = \begin{cases} 0.5p_0 \sin(2\pi ft)\left(1 - \cos\left(\frac{2\pi ft}{n_w}\right)\right) & t \in [0, T_w] \\ 0 & t \geq T_w \end{cases} \quad (8)$$

The output was registered in a node localized at the middle point at the opposite end. The exemplary numerical model of plate #4 with finite element mesh and applied excitation is presented in Fig. 3.

4. Results

4.1. Numerical simulations – Visualization of propagating wave

Fig. 4 presents the visualization of wave propagation in plates #1 and #4 characterized by extreme values of phase shift φ (see Eq. (7)). After wave excitation the high-amplitude antisymmetric mode propagates with comparable velocity in both plates. However, in plate #1 an additional low amplitude wave mode was triggered and it reached the plate edge first. Moreover, we can observe the differences in the amplitude. In the case of the plate with constant thickness, the amplitude decays exponentially [21], while if the thickness is variable the amplitude decreases with increasing plate thickness and increases with thickness decrease (Fig. 4, $t = 0.11$ ms).

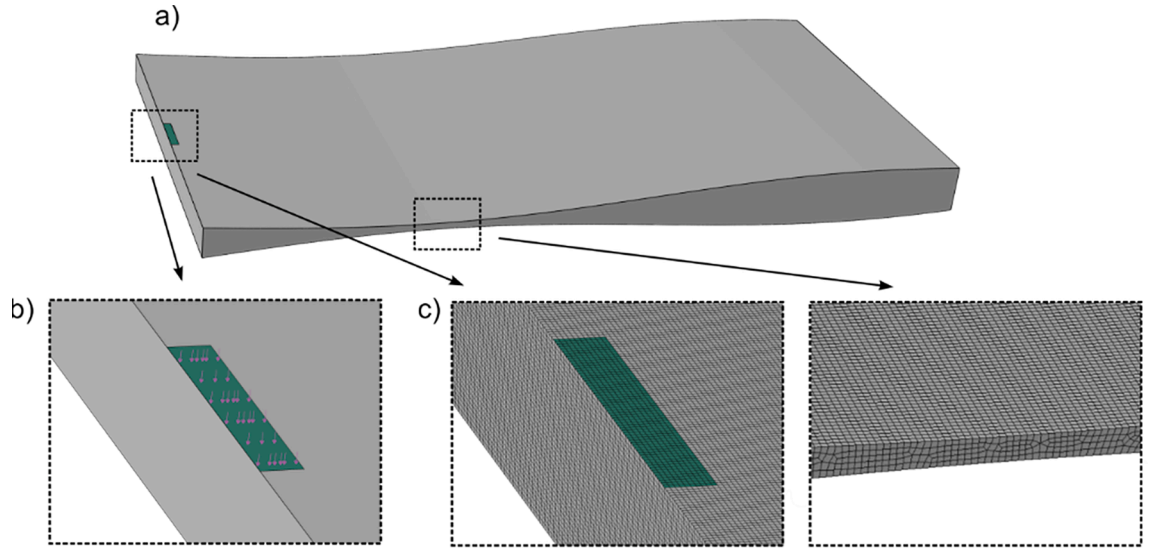

Fig. 3. Numerical simulations: a) model of plate#4 with b) applied pressure on the area corresponding to the area of the real transducers and c) finite element mesh at the edge of the plate and in the thinnest cross-section.

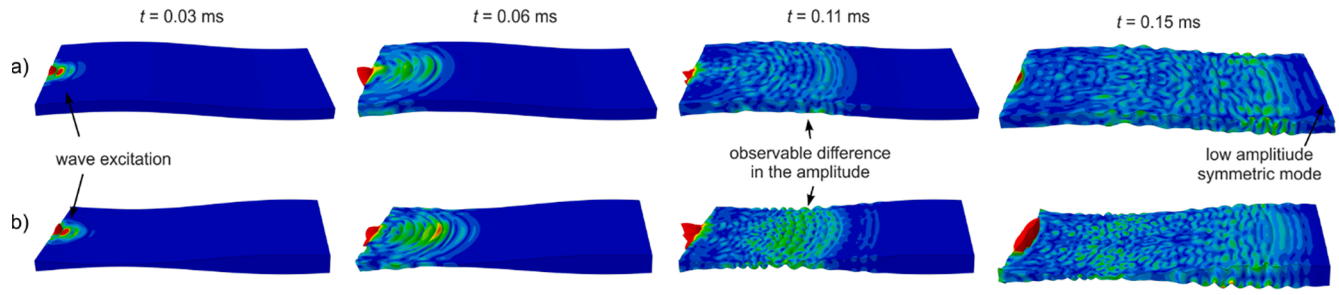

Fig. 4. Visualization of wave propagation in a) plate #1 and b) plate #4 at selected time instants.

4.2. *Signal reconstruction based on thickness histograms and exact plate geometry*

To verify the correctness of theoretical predictions, the time course of the signal corresponding to fundamental symmetric and antisymmetric mode was determined using two different approaches depicted in Fig. 5. The first approach (Fig. 5a) was based on an iterative procedure assuming that the signal from the previous step becomes the excitation in the next step. To reconstruct the signal, information about the exact thickness variability alongside the propagation path was required.

The second approach (Fig. 5b) incorporated only histograms of thickness distribution and Eq. (5). Fig. 5c presents the comparison of the signals obtained in two ways for exemplary chosen plate #3 and excitation of 200 kHz. It can be seen that in the case of A_0 mode the time variability of the displacement caused by wave motion was the same, which proved the correctness of the theoretical reasoning presented in Section 2. The slight deviations were noted for symmetric mode. The amplitudes are comparable, but the average velocity of the S0 mode was greater when the signal was determined using iterative derivation alongside plate length. The non-perfect correspondence of these two signals arises from the fact that the histogram is not an ideal representation of plate geometry. The accuracy of signal reconstruction based on the histogram depends on the number and the width of the bins. The effect is more visible for symmetric mode because it is more sensitive to thickness variations. Fig. 6 presents the dispersion curves for both modes determined for maximum and minimum thickness determined for plates #2, #3, and #4 (plate #1 is characterized by constant thickness, so the dispersion curves are not presented here). The differences in wave velocity in the case of antisymmetric mode vary from 0 to 100 m/s and for symmetric mode reach even 3000 m/s. Thus, the velocity of the S0 mode propagating alongside the plate varies significantly. In consequence, the discrepancies of exact thickness and the distance estimation resulting from non-perfect geometry description in the form of histogram together with significant velocity variabilities caused the differences between reconstructed signals to be more visible for S_0 mode. Nevertheless, the comparison of signals proves that the statistical description of geometry i.e. histograms of thickness distributions can be efficiently used to estimate the time variability of wave propagation signals.

To derive time-domain signals, in the first step the wave modes which can be excited in tested plates were identified. Fig. 7 presents the dispersion curves for an aluminum plate traced in the normalized frequency-thickness domain. Next, the extreme values of the frequency-thickness product have been calculated for each specimen by multiplying the excitation frequency by minimum and maximum plate thickness. The possible wave modes have been indicated by shaded areas. The frequency-product range, as well as the number of possible wave modes increases with increasing plate thickness variability.

Fig. 8 shows the theoretically derived time-domain signals, compared with numerical and experimental signals measured at the end of the plates for exemplary frequencies of 100 and 200 kHz, respectively. The theoretically derived signals were determined based on Eq. (5). Despite some differences between the signals obtained in different ways, the clear difference in the ToF for particular specimens caused by thickness variability is noticeable. Moreover, the ToF determined theoretically coincides well with numerical and experimental results, which proves the efficiency of signal reconstruction using histograms without the knowledge of the exact geometry. However, because the theoretical model was based on Rayleigh-Lamb dispersive equations derived for plane strain conditions, the theoretically determined signals do not contain edge reflections, which occur in numerical and experimental signals. Thus, they also seem to be less complex and much easier to interpret. Moreover, as presented in Fig. 7 the number of modes may

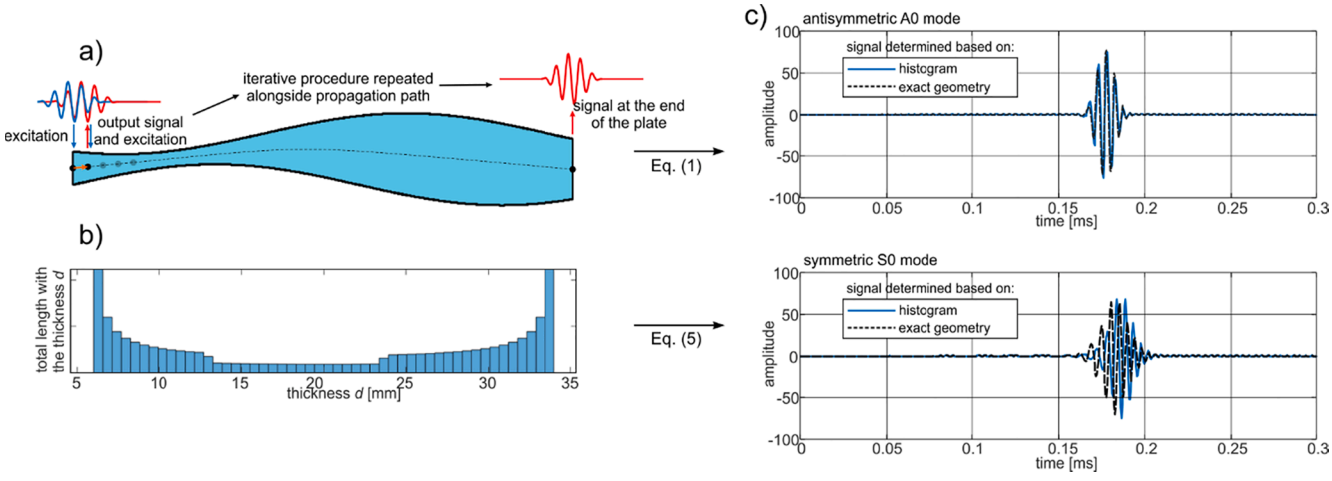

Fig. 5. The scheme of signal reconstruction based on plate geometry, dispersion relations and: a) iterative procedure repeated alongside propagation path, b) histogram of thickness distribution. Exemplary signals representing A_0 and S_0 mode in plate#3 presented in c) were determined for 200 kHz in two different ways and compared.

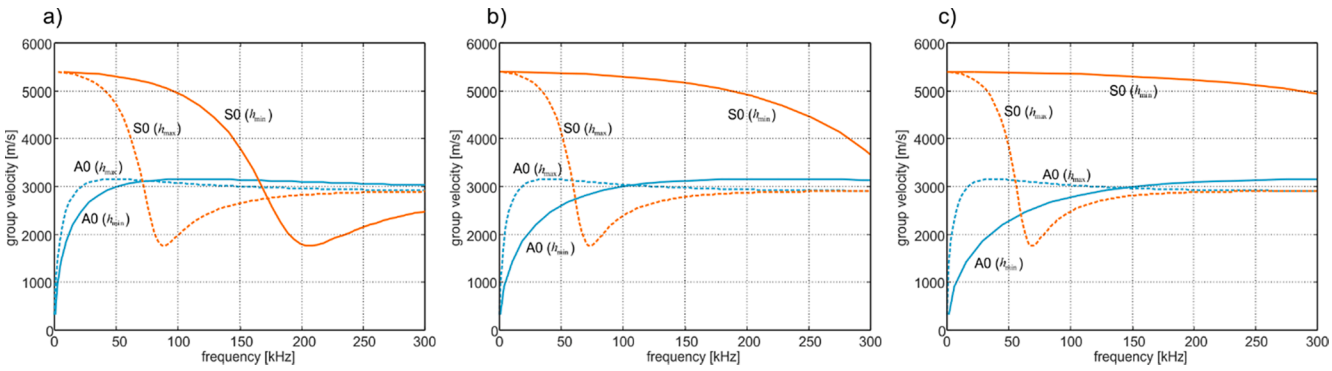

Fig. 6. Dispersion curves representing fundamental A_0 and S_0 modes traced for minimum and maximum thickness of a) plate #2, b) plate #3, c) plate #4.

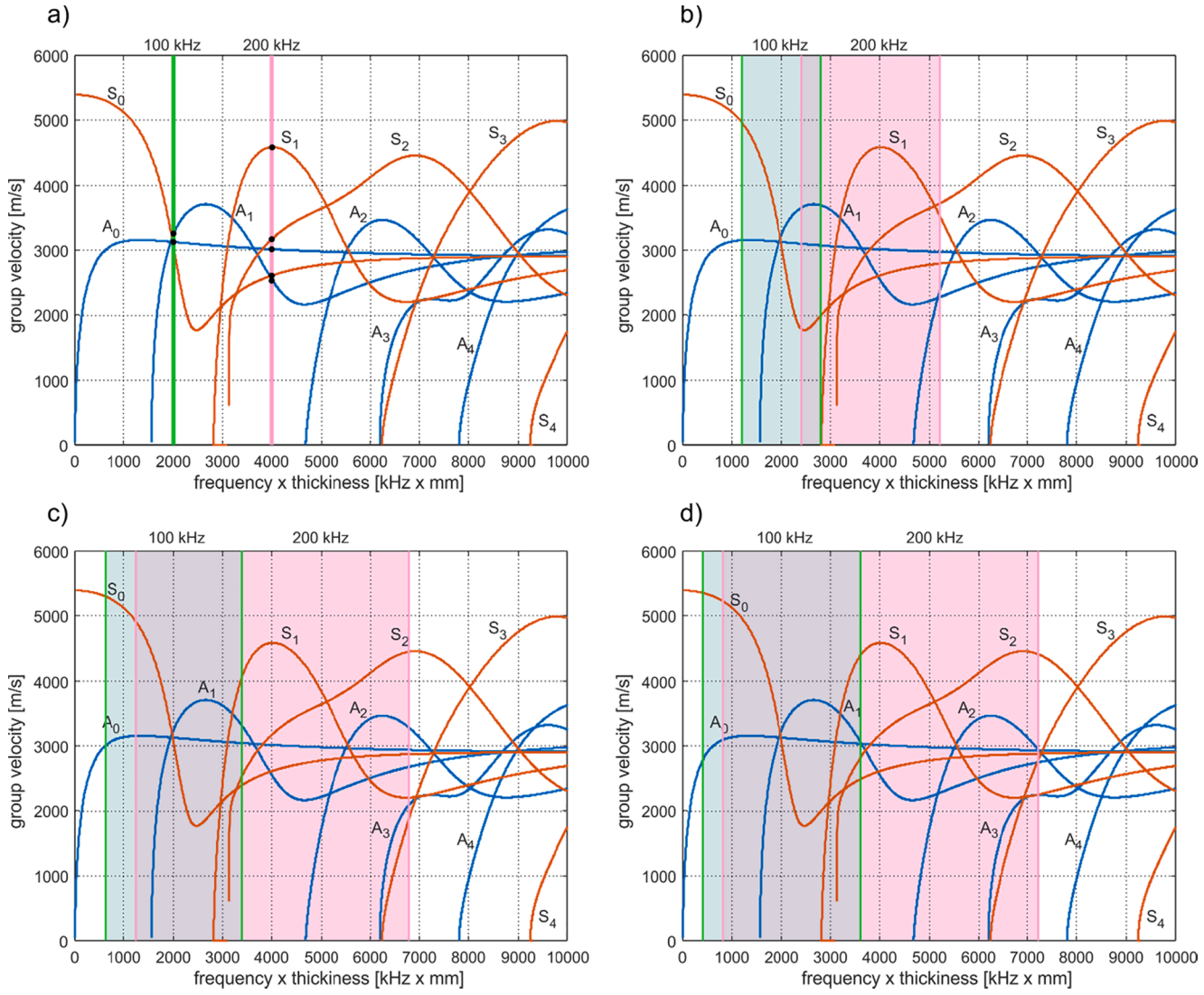

Fig. 7. Determination of wave modes that can occur in a) plate #1, b) plate #2, c) plate #3 and d) plate #4 for excitation frequency of 100 and 200 kHz.

vary considerably alongside the propagation path. The mode conversions and their reflections, especially in the case of plates #3 and #4, might influence the time course of registered signals. Nevertheless, the theoretical model allowed for the correct prediction of the order of modes registered at the end of the plate. One can see that in the case of excitation of 100 kHz the wave propagated the fastest in plate #1. For this frequency the velocities of all modes were comparable (Fig. 7a). However, 100 kHz is a central carrier, which means that the lower frequencies were also excited. The shortest ToF for this plate is the result of triggering symmetric S_0 mode characterized by relatively high velocity overlapping with slower antisymmetric A_0 mode. Usually, in the case of plates with constant thickness, depending on the direction of applied excitation, one mode type is characterized by much higher energy i.e. the perpendicular excitation triggers mainly antisymmetric modes and

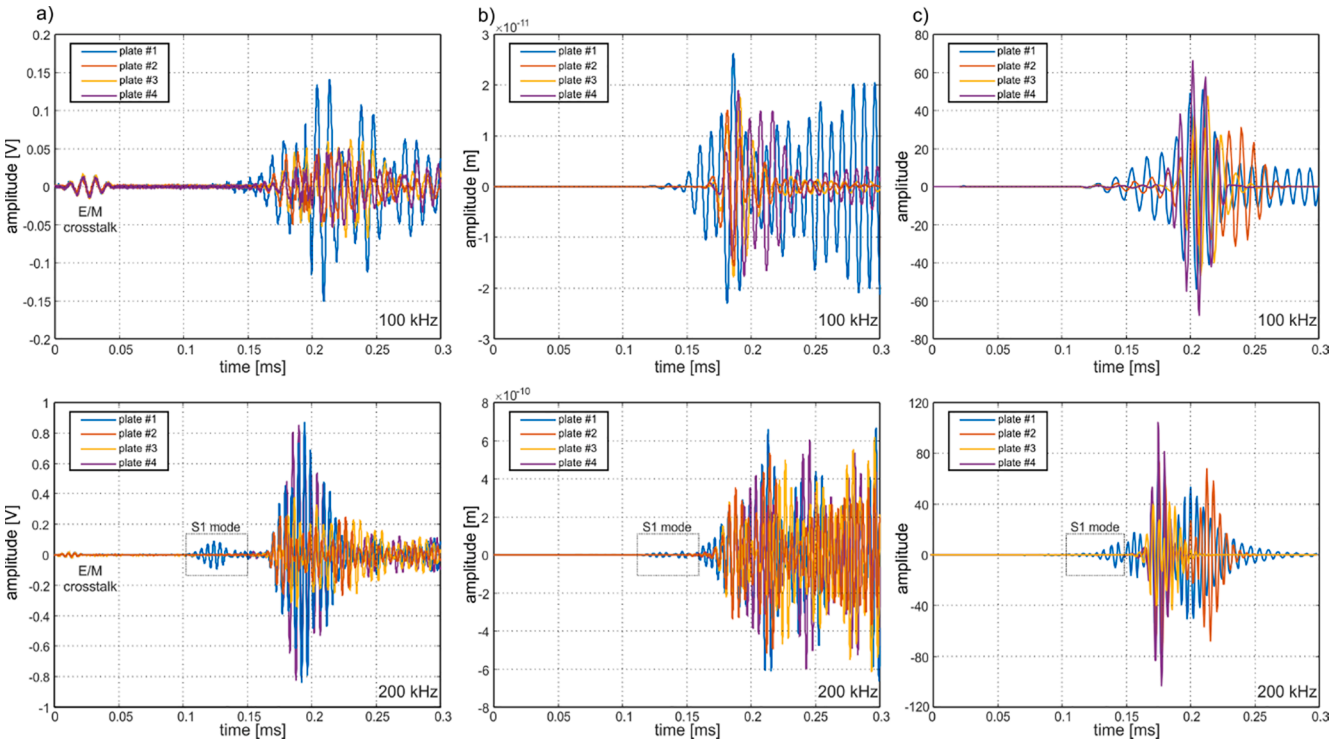

Fig. 8. Wave propagation signals collected for plates #1-#4 obtained a) experimentally, b) numerically and c) theoretically.

thus the possible symmetric mode has much lower amplitude. In consequence, the identification of particular modes is relatively straightforward. In the case of plates with irregular geometry, when the excitation is not perpendicular to the plate surface, the amplitudes of triggered modes can be comparable, which may result in difficulties in interpretation and wrong ToF or velocity estimation. In the considered case, taking into account only antisymmetric modes would be associated with significant velocity overestimation. In the context of damage localization purposes in specimens with complex geometry, it would result in incorrect determination of the defect position.

It is noteworthy that the histogram-based procedure supported by a fundamental equation describing the response of Lamb waves (Eq. (5)) allowed for the prediction of the propagation of higher-order modes which is visible, especially for frequency of 200 kHz and plate #1. In this case, the first registered mode was recognized as S_1 mode, which was characterized by the highest velocity for this frequency (Fig. 7a). The idea of using the histogram in predicting the higher-order modes propagation requires checking the number of possible wave modes for particular thicknesses. If we find that for a certain thickness the additional mode may exist, the signal from the previous step is treated as an excitation, while the exponential factor in Eq. (5) is determined for the new dispersion curve representing the higher-order mode. In the case of the histogram, the thickness always increases so the number of possible wave modes also only increases. If the procedure would allow for the possibility that the thickness in the following steps decreases (like in the case of the iterative procedure depicted in Fig. 5a), the higher-order mode would be converted into the lower-order mode if the frequency-thickness product would be below its cut-off frequency. This procedure has been applied in the case of each plate and all possible wave modes, which were summed up together, and finally the comparison of theoretical and experimental signals allowed for recognition of the first wave packet as S_1 mode propagating in plate #1. However, one of the limitations of the proposed procedure is the lack of possibility to predict the amplitude or the relations between the amplitudes of particular modes. So far developed phenomenological models do not provide information on how to predict the amplitude variability in a plate with non-constant thickness and multiple mode propagation [21]. In the presented case the amplitude of the S_1 mode has been artificially decreased to 30 % of its initial value only to keep the proportions between the amplitudes noted in experimental tests.

4.3. ToF variability in non-uniform sine-shaped plates

To analyze the influence of thickness variability on the ToF alongside the propagation path, the theoretical signals were calculated at each point with a 1 mm step. Next, the Hilbert transformation was incorporated to determine the signal envelope and calculate the ToF. The theoretically predicted ToF variability alongside propagation path for frequencies of 100, 150 and 200 kHz for fundamental antisymmetric and symmetric modes are presented in Fig. 9a and 9b, respectively. It can be seen that in the case of plate #1 the ToF increases linearly for both modes, which is associated with constant thickness and constant velocity. In other cases the ToF-distance becomes nonlinear, however, the nonlinearity is more visible for symmetric mode (Fig. 9b). In the case of antisymmetric mode, the deviations from linear patterns are negligible, which suggests it is less sensitive to thickness variability.

The potential velocity variability within the complex structure should be taken into account in wave-based damage detection and localization algorithms. As we can see, the ToF might depend not only on the distance between the transducers or obstacles but also on their exact location on the structure. The presented study demonstrates that it is possible to choose a wave mode that is insensitive to thickness variability, however, the non-uniform geometry always leads to triggering other wave modes affecting wave propagation signals and their characteristics.

5. Conclusions

The paper presents the results of numerical, experimental, and theoretical analysis of wave propagation in plates with variable thickness. The specially designed sine-shaped plates were tested. The following conclusions can be drawn based on the obtained results:

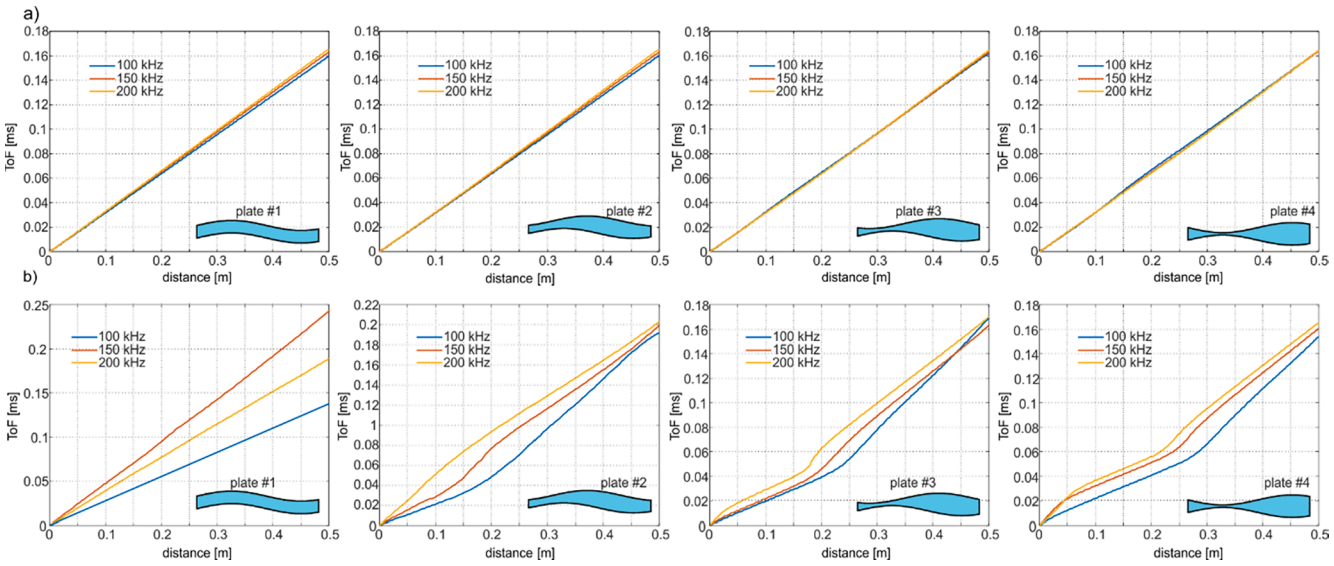

Fig. 9. ToF-distance relationship determined for different frequencies for a) A0 and b) S0 mode propagating in plates #1-#4 varying in thickness distribution.

- the time course of the signal can be derived using analytical equations of time variability of guided wave and the known geometry. Because the propagation velocity, as well as the shape of the wave packet, depend only on thickness distribution, and not on the exact shape of the plate, the signals can be efficiently determined using histograms. The statistical information about the geometry allowed for the prediction of the presence of higher-order modes. Moreover, the ToF of guided waves in different plates for variable excitation frequency was predicted correctly;
- the irregular geometry leads to significant velocity variability within the structure. Despite the possibility to choose a wave mode insensitive to thickness variability, the irregular geometry leads to triggering more than one mode, which significantly hinders the interpretation of the signals. Therefore, the common approach based on using the average wave velocity e.g. for damage localization purposes in plates characterized by variable thickness may result in significant errors.

In the next steps, it is planned to consider the inverse problem aimed at determining the histogram of thickness distribution based on registered signals.

Declaration of Competing Interest

The authors declare that they have no known competing financial interests or personal relationships that could have appeared to influence the work reported in this paper.

Data availability

Data will be made available on request.

Acknowledgement

The first author greatly acknowledges the support of the Foundation for Polish Science (FNP).

References

[1] D.J. Luis, C. Trillo, A. Doval, J.L. Fernandez, Determination of thickness and elastic constants of aluminum plates from full-field wavelength measurements of single-mode narrowband Lamb waves, J. Acoust. Soc. Am. 124 (3) (2008) 1477–1489.
[2] J.L. Rose, Ultrasonic Guided Waves in Solid Media 9781107048 (2014) 1–512.
[3] H. Lamb, On waves in an elastic plate, Proc. R. Soc. A Math. Phys, Eng. Sci. 93 (648) (1917) 114–128.
[4] B. Zima, K. Woloszyk, Y. Garbatov, Corrosion degradation monitoring of ship stiffened plates using guided wave phase velocity and constrained convex optimization method, Ocean Eng. 253 (2022), 111318.
[5] A. Farhidzadeh, S. Salamone, Reference-free corrosion damage diagnosis in steel strands using guided ultrasonic waves, Ultrasonics 57 (2015) 198–208.
[6] J. Moll, Damage localization in composite structures with smoothly varying thickness based on the fundamental antisymmetric adiabatic wave mode, Ultrasonics 71 (2016) 111–114.
[7] V. Pagneux, A. Maurel, Lamb wave propagation in elastic waveguides with variable thickness, in: Proc. R. Soc, 462, Ser. A, London, 2006, pp. 1315–1339.
[8] M.-C. El-Kettani, F. Luppé, A. Guillet, Guided waves in a plate with linearly varying thickness: experimental and numerical results, Ultrasonics 42 (1–9) (2004) 807–812.
[9] L. Moreau, J.G. Minonzio, M. Talmant, P. Laugier, Measuring the wavenumber of guided modes in waveguides with linearly varying thickness, J. Acoust. Soc. Am. 135 (5) (2014) 2614–2624.
[10] C. Höhne, J. Prager, Simulation of ultrasound propagation in waveguides with non-constant thickness by a multimodal approach, Forum Acusticum (2014) 1–6.
[11] C. Höhne, Multimodal Approach for the Numerical Simulation of Ultrasonic Guided Waves in Cylindrical Structures of Non-Constant Thickness, Technischen Universität Cottbus-Senftenberg, 2016. PhD thesis,.
[12] L. De Marchi, A. Marzani, N. Speciale, E. Viola, Prediction of pulse dispersion in tapered waveguides, NDT & E Int. 43 (3) (2010) 265–271.
[13] L. De Marchi, A. Marzani, M. Miniaci, A dispersion compensation procedure to extend pulse-echo defects location to irregular waveguides, NDT & E Int. 54 (2013) 115–122.
[14] Q. Deng, Z. Yang, Propagation of guided waves in bonded composite structures with tapered adhesive layer, Appl. Math. Model. 35 (11) (2001) 5369–5381.
[15] J. Moll, T. Wandowski, P. Malinowski, M. Radzienski, M.S. Opoka, W. Ostachowicz, Experimental analysis and prediction of antisymmetric wave motion in a tapered anisotropic waveguide, J. Acoust. Soc. Am 138 (2015) 299–306.
[16] B. Zima, Determination of stepped plate thickness distribution using guided waves and compressed sensing approach, Measurement 196 (2022) 111221.
[17] K. Neuschwander, J. Moll, V. Memmolo, M. Schmidt, M. Bücker, Simultaneous Load and Structural Monitoring of a Carbon Fiber Rudder Stock: Experimental Results from a Quasi-Static Tensile Test, J. Intell. Mater. Syst. Struct. 30 (2019) 272–282.
[18] F. Moser, L.J. Jacobs, J. Qu, Modeling elastic wave propagation in waveguides with finite element method, NDT&E Int. 32 (1999) 225–234.
[19] D. Alleyne, P. Cawley, A two-dimensional Fourier transform method for measurement of propagating multimode signals, J. Acoust. Soc. Am. 89 (3) (1999) 1159–1168.
[20] R. Courant, K. Friedrichs, H. Lewy, On the partial difference equations of mathematical physics, IBM 11 (1967) 215–234.
[21] B. Zima, R. Kędra, Detection and size estimation of crack in plate based on guided wave propagation, Mech. Syst. Sig. Process. 142 (2020), 106788.